Applied and Environmental Microbiology, June 2006, p. 3908–3915 Vol. 72, No. 6
0099-2240/06/$08.00+0 doi:10.1128/AEM.02429-05

Quantifying the Significance of Phage Attack on Starter Cultures: a Mechanistic Model for Population Dynamics of Phage and Their Hosts Isolated from Fermenting Sauerkraut§

P. Mudgal,† F. Breidt, Jr.,* S. R. Lubkin,‡ and K. P. Sandeep†

U.S. Department of Agriculture, Agricultural Research Service, North Carolina Agricultural Research Service, Department of Food Science, Box 7624, North Carolina State University, Raleigh, North Carolina 27695-7624

Received 13 October 2005/Accepted 21 March 2006

We investigated the possibility of using starter cultures in sauerkraut fermentation and thereby reducing the quantity of salt used in the process. This, in turn, would reduce the amount of waste salt that would enter in our water resources. Phage, naturally present in sauerkraut fermentation, could potentially affect the starter cultures introduced. Thus, a mechanistic mathematical model was developed to quantify the growth kinetics of the phage and starter cultures. The model was validated by independent experiments with two *Leuconostoc mesenteroides* strains isolated from sauerkraut and their corresponding phage. Model simulations and experimental evidence showed the presence of phage-resistant cell populations in starter cultures which replaced phage-sensitive cells, even when the initial phage density (P_0) and multiplicity of infection (MOI) were low ($P_0 < 1 \times 10^3$ PFU/ml; MOI $< 10^{-4}$) in the MRS media. Based on the results of model simulation and parameter optimization, it was suggested that the kinetic parameters of phage-host interaction, especially the adsorption rate, vary with the initial phage and host densities and with time. The model was validated in MRS broth. Therefore, the effects of heterogeneity and other environmental factors, such as temperature and pH, should be considered to make the model applicable to commercial fermentations.

Traditionally, sauerkraut fermentation is carried out by a small population of lactic acid bacteria (LAB) indigenous to cabbage in the presence of 2 to 3% salt (24). Sauerkraut fermentation is carried out in two stages, a heterofermentative stage followed by a homofermentative stage. *Leuconostoc mesenteroides* initiates the early heterofermentative stage and is primarily responsible for the quality characteristics, such as flavor and aroma, of sauerkraut (22). Salt serves as a selecting agent for LAB and thus is an important factor in deciding the microbial succession during sauerkraut fermentation. During the fermentation process, excess brine is discharged in effluents from processing plants. Due to the environmental concerns about waste salt disposal and the associated economic issues, it may be desirable to reduce the salt concentration by 50% or more. To ensure quality with low-salt fermentations, starter cultures may be needed to maintain the desired flavor and texture of the finished product.

In previous studies, *Leuconostoc* species have been used as starter cultures for sauerkraut fermentations. The starter cultures were found to prolong the heterolactic fermentation, which is responsible for the characteristic flavor and aroma of sauerkraut (4, 13). Recent studies have investigated the genetics and ecology of bacteriophage from fermentating sauerkraut (20, 30). Phage active against several LAB have been isolated from commercial fermentations, including *L. mesenteroides*, which is a potential starter culture for sauerkraut fermentation (20, 30). These studies raised the possibility that phage may interfere with the use of starter cultures in low-salt vegetable fermentations. To address this question, we have developed and validated a mathematical model for the population dynamics of phage and prospective starter cultures. The objective was to quantitatively determine the impact of phage on the starter culture under various initial conditions of phage and host cell densities. A model consisting of a system of delay differential equations has been developed and validated using two *Leuconostoc* strains and their corresponding phage isolated from commercial sauerkraut fermentation. The model was validated by comparing the predicted and experimentally determined phage-host densities over time and also by comparing predicted and experimentally determined kinetic parameters defining phage-host interaction, including bacterial growth rates, carrying capacity, latent period, burst size, and adsorption rate coefficient.

Phage-host interaction has been studied mathematically for decades (9, 10), and interesting features are still being discussed and studied. These studies include ecological models of phage and bacteria (18, 21) and models evaluating the potential of phage as therapeutic agents (14, 17, 23, 26). However, very few phage-host models for population dynamics exist that have also been validated, such as those by Levin and Bull (17) and Middleboe (21), or have been analyzed mathematically (23). Some phage-host modeling studies have focused on particular aspects of phage-host interaction models, such as the dependence of parameters on the growth rate (25), a model for

* Corresponding author. Mailing address: U.S. Department of Agriculture, Agricultural Research Service, North Carolina Agricultural Research Service, Department of Food Science, Box 7624, North Carolina State University, Raleigh, NC 27695-7624. Phone: (919) 513-0186. Fax: (919) 513-0180. E-mail: breidt@ncsu.edu.

† Present address: Department of Food Science, Box 7624, North Carolina State University, Raleigh, NC 27695-7624.

‡ Present address: Department of Mathematics, North Carolina State University, Box 8205, Raleigh, NC 27695-8205.

§ Paper no. FSR05-26 of the Journal Series of the Department of Food Science, North Carolina State University, Raleigh, NC 27695-7624.

the lysis of phage (27), phage growth dependence on the physiology of cells (12), and prediction of mature phage inside and after lysis of a cell by a single phage infection (26). Some models contain too many parameters, which may make them difficult to validate.

In the present study, a semimechanistic model with easily measurable, biologically meaningful parameters was developed using four delay differential equations. The model accurately predicts phage-host numbers over significantly large periods of time (10 h) and has been validated with two phage-host systems using different initial phage and host densities. A separate variable for resistant cells was added to the model to accurately predict the results. An adsorption rate coefficient, which varies with time, was used in the model in place of an adsorption rate constant. Parameters were optimized for two phage-host systems and also compared with experimental values. In this study, some interesting features about the variation of parameters (especially the adsorption rate coefficient) with time and their interdependence have been noted, and they merit further investigation.

MATERIALS AND METHODS

Bacterial strains, phage, and media. The two phage-host systems used in this study were (i) *L. mesenteroides* 1-A4 and its corresponding phage, 1-A4, and (ii) *Leuconostoc pseudomesenteroides* 3-B11 and phage 3-B11. Bacterial strains and phage were previously isolated from commercial fermenting sauerkraut (20) and were obtained from the U.S. Department of Agriculture Agricultural Research Service Food Fermentation Laboratory Culture Collection (Raleigh, NC). All bacterial stocks were kept at −84°C in MRS broth (Difco Laboratories, Detroit, MI) containing 16% (vol/vol) glycerol. Bacterial cells were grown at 30°C in MRS broth supplemented with 5 mM $CaCl_2$. To generate phage lysates, an early log phase cell culture was prepared by inoculating 5 ml of MRS medium prewarmed to 30°C with a 1% inoculum from a 15-h overnight culture. The cells were incubated for 3 to 5 h and then inoculated at a multiplicity of infection (MOI; ratio of PFU/CFU) between 0.01 and 0.05 with the corresponding phage, and 5 mM $CaCl_2$ was added. The cell-phage mixture was then incubated at 30°C for 7 h. After 7 h, the cell-phage suspension was filter sterilized using a 0.45-μm syringe filter, and the supernatant was stored at 4°C.

Determining phage and bacterial concentrations. The bacterial concentration in the media was determined using a Spiral plater (Autoplate 4000; Spiral Biotech, Inc., Bethesda, MD) and cell suspensions diluted appropriately with sterile saline (0.85% NaCl). Viable-cell counts were performed using an automatic colony counter (Protos Plus; Bioscience International, Rockville, MD). The phage titer was determined by using a standard double-layer agar plate method similar to that of Adams (2). After appropriate dilution with saline, 0.1 ml of phage sample, 0.1 ml of actively growing culture (10^8 CFU/ml), and 30 μl of 1 M $CaCl_2$ were added to 3 ml of soft agar (maintained at 48°C). The mixture was overlaid on MRS agar plates and incubated overnight at 30°C to enumerate plaques.

Determination of model parameters. (i) Growth rates. Bacterial growth rates were calculated from the optical density (OD) measurements using a microtiter plate reader (ELX 808 IU Ultra Microplate Reader; Biotek Instruments Inc., Winooski, VT). Twenty microliters of the overnight culture (17 h) was diluted with 180 μl of MRS medium and overlaid with 75 μl of mineral oil in microtiter plate wells (6). These fermentations were placed inside the microtiter plate reader. The internal temperature was maintained at 30°C by placing the microtiter plate reader in a custom heating-cooling incubator (Price Scientific Services, Inc., Durham, NC). The optical density was monitored every hour up to 24 h. A temperature-recording device (OM-3000 MAS Data Logger; Omega Engineering Inc., Stanford, CT) with thermocouples placed inside the microtiter plate reader was used to monitor the temperature of fermentations. Eight replicates were performed for both bacteria, *L. mesenteroides* 1-A4 and *L. pseudomesenteroides* 3-B11. The data were analyzed using the Gompertz model to calculate specific growth rates (7). The growth rates for both bacteria were determined in MRS medium supplemented with 0, 1, 2, 5, 8, 10, 12, and 15 mM $CaCl_2$. Above 15 mM, turbidity from $CaCl_2$ prevented OD measurements.

(ii) Burst size and latency. One-step growth experiments were performed as defined by Ellis and Delbruck (11) to determine the latent period and burst size.

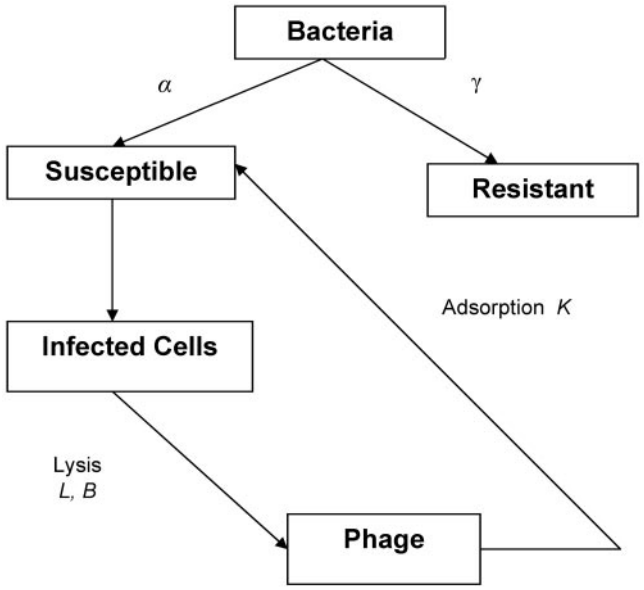

FIG. 1. Diagram of basic mechanism of phage-host model (α, growth rate of susceptible bacteria; γ, growth rate of resistant bacteria; *L*, latent period; *B*, burst size; and *K*, adsorption rate coefficient).

Briefly, host cells were infected with phage in the early exponential phase (OD = 0.3) at an MOI of ≈0.04 for *L. pseudomesenteroides* 3-B11 and at an MOI of ≈0.25 for *L. mesenteroides* 1-A4. Five millimolar calcium chloride was added to aid adsorption. After allowing adsorption for 10 min, the infected cells were pelleted by centrifugation (RC-5B centrifuge; Sorvall, Wilmington, DE) at 8,000 × *g* for 5 min at 4°C. The pelleted infected cells were then resuspended in fresh MRS broth supplemented with 5 mM $CaCl_2$. Samples were taken every 5 to 10 min up to 2 h and were immediately titered by the double-layer agar plate method. Three independent replicates of one-step growth experiments were performed for both phage 1-A4 and phage 3-B11 to observe variation in the parameters, including the latent period and burst size. The data were fitted with a four-parameter symmetric sigmoidal model. Nonlinear regression was performed using Sigmaplot (version 8.0) to calculate the latent period and burst size.

(iii) Adsorption rates. Adsorption experiments were performed with a modification of the procedure of Ellis and Delbruck (11). A 6-ml culture of bacterial cells grown to early log phase was infected with phage as described above, and then 5 mM $CaCl_2$ was added. At the indicated time intervals, 0.6-ml aliquots were removed and filtered using a 0.45-μm syringe filter to obtain free phage in the filtrate. The filtered samples containing free phage were then titered immediately using the double-layer agar plate method. Independent adsorption experiments were performed by varying the optical densities of cells at the time of infection, and also the multiplicity of infection. For *L. mesenteroides* 1-A4, adsorption experiments were performed at optical densities of 0.20, 0.15, and 0.22 and at MOIs of 0.13, 0.09, and 0.1, respectively. For *L. pseudomesenteroides* 3-B11, adsorption experiments were performed at optical densities of 0.2 and 0.3 and at MOIs of 0.03 and 0.02, respectively. The data were fitted with a two-parameter exponential-decay model using Sigmaplot. The adsorption rate coefficient was determined at time zero using initial cell and phage densities.

(iv) Model description. A schematic diagram of the model is presented in Fig. 1. Initially, our model consisted of three variables (*S*, *P*, and *I*; see below for descriptions of the variables) using ordinary differential equations without time delay for phage multiplication, similar to previous phage-host models (3, 8). Based on studies of phage-host kinetics, the model was modified to incorporate a delay term ($t - L$) to represent phage maturation. In addition, the adsorption rate was found to vary with time, which led to the incorporation of a step function (*H*). A fourth variable (*M*), representing the density of resistant cells, was added because cell growth was observed in the presence of viable phage. Resistant cells were subsequently identified experimentally (data not shown). The resulting model consists of a system of delay differential equations for four state variables

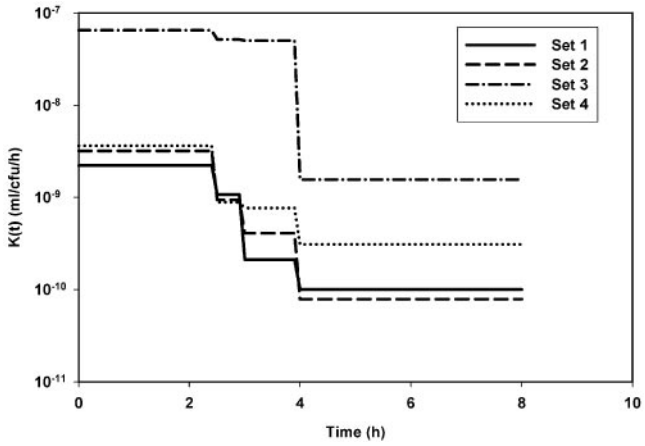

FIG. 2. Time dependence of the adsorption rate coefficient, $K(t)$, as determined by parameter fitting for *L. mesenteroides* 1-A4 and phage 1-A4 (Table 2).

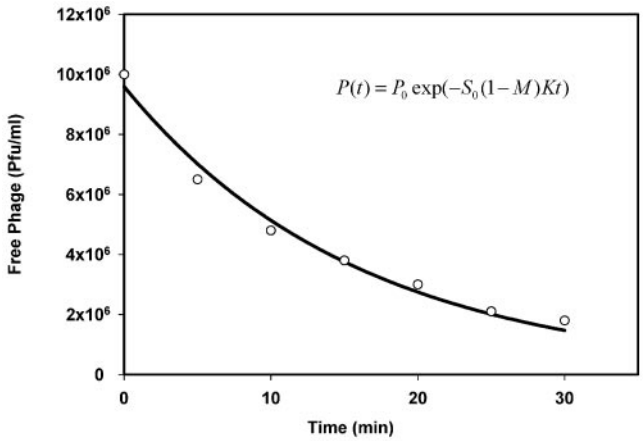

FIG. 4. Free-phage decay curve for adsorption of phage 1-A4 to *L. mesenteroides* 1-A4 in MRS medium supplemented with 5 mM $CaCl_2$ at 30°C. The data are fitted to the function $P(t) = P_0 \exp[-S_0(1 - M)K(t)t]$. $S_0 = 7.98 \times 10^7$ CFU/ml initial MOI, $M = 0.13$, and $K = 5.4 \times 10^{-8}$ ml/CFU/h.

in time t: $S(t)$, $M(t)$, and $I(t)$, the densities of susceptible, resistant, and infected cells, and $P(t)$, the density of free phage.

$$\frac{dS}{dt} = \alpha S\left(1 - \frac{S + I + M}{C}\right) - K(t)S\,P$$

$$\frac{dI}{dt} = K(t)SP - H(t - L)K(t - L)S(t - L)P(t - L)$$

$$\frac{dP}{dt} = -K(t)SP + BH(t - L)K(t - L)S(t - L)P(t - L)$$

$$\frac{dM}{dt} = \gamma M\left(1 - \frac{S + I + M}{C}\right)$$

The model parameters are as follows: α, the growth rate of susceptible cells; γ, the growth rate of resistant cells; C, the maximum cell density; B and L, the burst size and latent period of the phage, respectively; and K, the adsorption rate coefficient. The step function, $H(t - L)$, is 0 for a t of $<L$ and 1 for a t of $>L$. The value of K was found to be time dependent, so the following step function was used to vary the adsorption rate coefficient in time (Fig. 2):

$$0 \le t < 2.5, K = K_0; 2.5 \le t < 3, K = K_1; 3 \le t < 4, K = K_2; 4 \le t, K = K_3.$$

The assumptions for the model were as follows. (i) The medium is homogeneous and mixed, so that the rate of encounters between bacteria and phage follows the law of mass action. (ii) Infected cells do not divide. (iii) A cell can be infected by only one phage. (iv) In the absence of phage, the bacterial population can grow only to the carrying capacity, C. (v) The adsorption rate coefficient, K, varies with time depending on the physiological state of the cells and cell densities. (vi) All phage are capable of binding to and infecting the cells. (vii) Phage cannot adsorb to anything but susceptible cells. (viii) All adsorbed phage reproduce by bursting their cells with a fixed latent period and burst size.

Validation of the model for the two phage-host systems studied, *L. mesenteroides* 1-A4–phage 1-A4 and *L. pseudomesenteroides* 3-B11–phage 3-B11, was carried out as follows. Early-log-phase cells were prepared as described above, infected with the phage at the indicated MOIs, and incubated at 30°C in 6 ml MRS broth containing 5 mM $CaCl_2$. Samples (200-μl aliquots) were taken from the phage-cell suspension at 20- to 30-min intervals. Bacterial-cell counts and phage titers were determined as described above. The initial cell and phage concentrations for these validation experiments were as follows: *L. mesenteroides* 1-A4 and phage 1-A4, set 1, $S_0 = 8 \times 10^7$ CFU/ml, $P_0 = 8.2 \times 10^6$ PFU/ml; set 2, $S_0 = 7.5 \times 10^7$ CFU/ml, $P_0 = 2 \times 10^6$ PFU/ml; set 3, $S_0 = 2.66 \times 10^7$ CFU/ml, $P_0 = 2 \times 10^7$ PFU/ml; set 4, $S_0 = 7.5 \times 10^5$ CFU/ml, $P_0 = 1.4 \times 10^3$ PFU/ml; *L. pseudomesenteroides* 3-B11 and phage 3-B11, set 1, $S_0 = 4.8 \times 10^7$ CFU/ml, $P_0 = 1.31 \times 10^5$ PFU/ml; set 2, $S_0 = 2.92 \times 10^6$ CFU/ml, $P_0 = 2.92 \times 10^2$ PFU/ml, where S_0 is the initial density of susceptible cells and P_0 is the initial density of

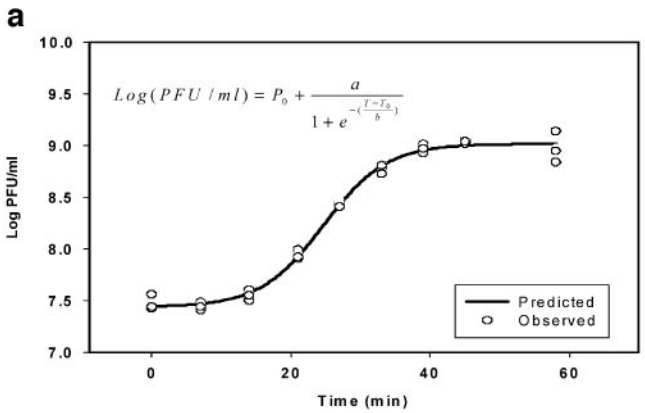

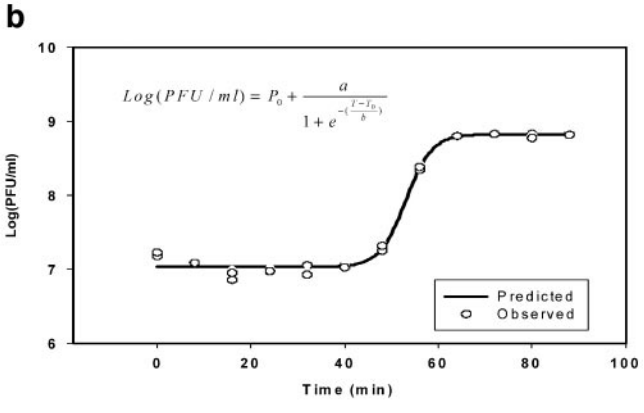

FIG. 3. One-step growth curve of (a) *L. mesenteroides* 1-A4 and phage 1-A4 and (b) *L. pseudomesenteroides* 3-B11 and phage 3-B11 in MRS medium with 5 mM $CaCl_2$ at 30°C. T_0 is the time at maximal slope; P_0 is log phage density at time zero; burst size, B, is calculated as 10^a, or $\alpha = \log(B)$; b is a time characteristic of the rise of the sigmoidal curve; latent period, L, is equal to $T_0 - b$. (a) $B = 37$, $T_0 = 20$ min; (b) $B = 62$, $T_0 = 51$ min.

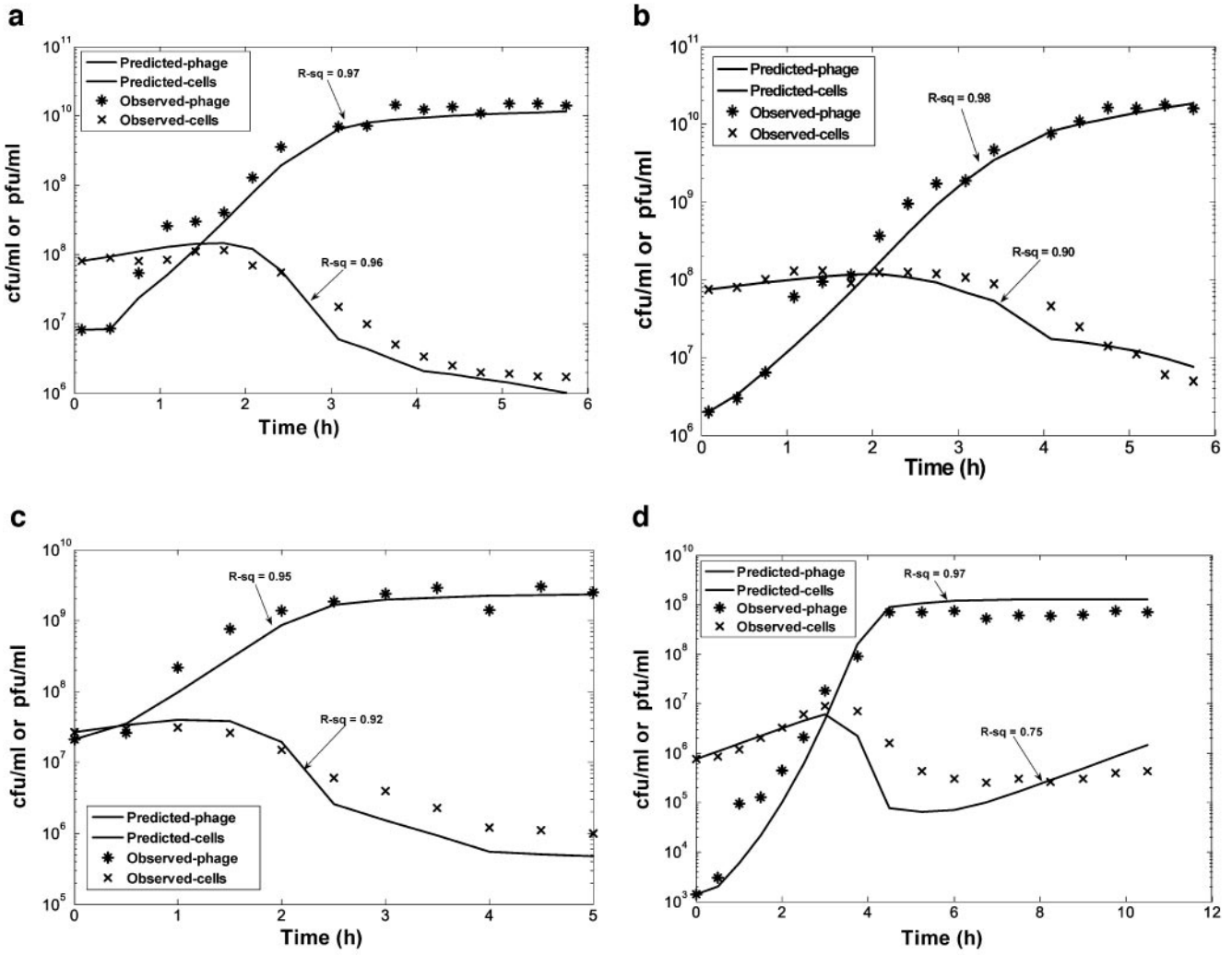

FIG. 5. Validation results for different sets of *L. mesenteroides* 1-A4 and phage 1-A4. The parameters used are average values of parameters obtained after parameter optimization for individual sets. The R^2 (R-sq) values for both phage and cell predictions shown were calculated for observed and predicted phage data and cell density data. (a) $S_0 = 8 \times 10^7$ CFU/ml, $P_0 = 8.2 \times 10^6$ PFU/ml; (b) $S_0 = 7.5 \times 10^7$ CFU/ml, $P_0 = 2 \times 10^6$ PFU/ml; (c) $S_0 = 2.66 \times 10^7$ CFU/ml, $P_0 = 2 \times 10^7$ PFU/ml; (d) $S_0 = 7.5 \times 10^5$ CFU/ml, $P_0 = 1.4 \times 10^3$ PFU/ml.

phage. The initial density of infected cells in all of the experiments was 0 ($I_0 = 0$), and the initial density of resistant cells (M_0) was considered to be a fraction of S_0. This ratio was set at $1{:}10^6$ for *L. mesenteroides* 1-A4 and $1{:}10^5$ for *L. pseudomesenteroides* 3-B11 (as described below).

Spiral plate counts gave the sum of susceptible and resistant bacterial counts, $S + M$, and plaque assays gave the sum of infected cells and free phage, $I + P$, in the solution. These values were compared with the corresponding predicted values from the model. All statistics were applied to the log-transformed values of total phage and cell concentrations. The sum of squared error term (SSE) was calculated from the observed and predicted numbers for both cells and phage. The total sum of squared error [SSE(T)] was obtained by adding SSE (cells) and SSE (phage). Parameter optimization by SSE(T) minimization was carried out using a random-walk algorithm (5) with a MATLAB (version 6.5; The MathWorks Inc., Natik, MA) implementation of the model. Parameter optimization was done for each set of validation experiments and also for multiple sets taken together. Parameter optimization in every case was verified by varying the initial parameter vector and number of iterations. Finally, variation in parameters (the coefficient of variation [% CV]) within and among different sets of validation experiments was calculated for both phage-host combinations using the Statistics tool in Sigmaplot. All measurements below are reported as mean ± standard deviation (SD).

RESULTS

Bacterial growth rates. The specific growth rate of *L. mesenteroides* 1-A4 in MRS medium supplemented with 5 mM $CaCl_2$ was 0.30 ± 0.01 h^{-1}, and the growth rate of *L. pseudomesenteroides* 3-B11 was 0.32 ± 0.01 h^{-1} at 30°C. The growth rates of resistant cells, calculated from the optical density data, were found to be 0.30 h^{-1} and 0.27 h^{-1} for *L. mesenteroides* 1-A4 and *L. pseudomesenteroides* 3-B11, respectively. The maximum cell densities were found to be 9×10^8 CFU/ml for *L. mesenteroides* 1-A4 and 8×10^8 CFU/ml for *L. pseudomesenteroides* 3-B11 in MRS medium supplemented with 5 mM $CaCl_2$. For *L. mesenteroides* 1-A4, the growth rate decreased from 0.33 ± 0.005 h^{-1} at 0 mM $CaCl_2$ to 0.27 ± 0.009 h^{-1} at 15 mM $CaCl_2$. This difference was significant ($P \ll 0.0001$). It was observed that the bacterial growth rate remained nearly constant (≈0.300) in a range of concentration from 2 to 8 mM

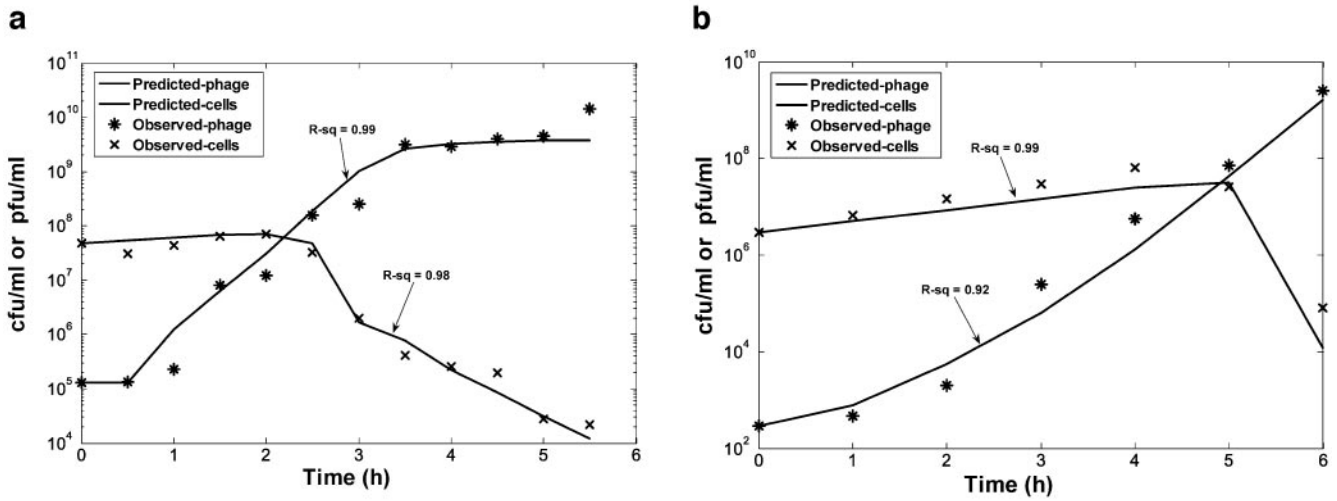

FIG. 6. Validation results for different sets of *L. pseudomesenteroides* 3-B11 and phage 3-B11. The parameters used are average values of parameters obtained after parameter optimization for individual sets. The R^2 (R-sq) values for both phage and cell predictions shown were calculated for observed and predicted phage data and cell density data. (a) $S_0 = 4.8 \times 10^7$ CFU/ml, $P_0 = 1.31 \times 10^5$ PFU/ml; (b) $S_0 = 2.92 \times 10^6$ CFU/ml, $P_0 = 2.92 \times 10^2$ PFU/ml.

$CaCl_2$ for *L. mesenteroides* 1-A4. No significant difference was found between these groups. Similarly, for *L. pseudomesenteroides* 3-B11, the growth rate decreased from 0.35 ± 0.006 h^{-1} at 0 mM to 0.28 ± 0.01 h^{-1} at 15 mM $CaCl_2$. This difference was also significant ($P \ll 0.0001$).

Phage kinetics. The burst size for phage 1-A4 ranged from 11 to 37, with a mean value of 24 and SD of 13. For phage 3-B11, the latent period varied from 39 to 51 min, with a mean of 44 min and SD of 6.25 min, and the burst size was found to vary from 37 to 62, with a mean value of 47 and SD of 13. One-step growth curves are shown in Fig. 3a and b for phage 1-A4 and phage 3-B11, respectively. The mean values of the adsorption rate coefficient for various initial cell and phage numbers were found to be 5.5 ± 0.023 × 10^{-8} ml/CFU/h for phage 1-A4 and 5.05 ± 1.2 × 10^{-8} ml/h for phage 3-B11. A representative plot of free-phage decay with time due to adsorption of phage is shown in Fig. 4.

Parameter optimization and validation. Using parameter values obtained from optimization of individual sets, the model predictions fit the observed phage and cell density data with high R^2 values (≈0.95). Validation of the model comparing predicted and observed cell and phage counts is shown in Fig. 5a to d for *L. mesenteroides* 1-A4 using the initial conditions in sets 1 to 4, respectively, as described above. Similarly, Fig. 6a and b shows the validation data using the initial conditions described above for *L. paramesenteroides* sets 1 and 2, respectively. The predicted values in these figures were obtained using the average values of parameters from the results of parameter optimization. The % CV was determined among the results of multiple iterations of parameter optimization for individual sets to check for consistency of the results. Parameter values were found to be consistent with a CV of less than 40% for most of the parameters. Individual R^2 values were not normalized for the number of data points, as all conditions had roughly the same number of points. All statistics were calculated in MATLAB. Parameters obtained numerically from parameter optimizations of different sets of phage-host systems 1-A4 and 3-B11 were compared with the corresponding experimentally determined values, along with their standard deviations (see Table 3).

Parameter optimization and modeling. Parameter optimization was done to find a common set of parameters for each phage-host combination to be used for all initial conditions tested. Each row in Table 1 corresponds to a parameter vector, resulting in the least possible SSE(T) for observed and predicted data using parameters after optimization of given sets simultaneously, as indicated in the leftmost column of Table 1. It was possible to find a single parameter set, which predicted with high R^2 values ($R^2 \approx 0.97$) and low SSE(T) (≈2.0) values for sets with similar initial cell and phage densities (set 1 and set 2, $S_0 \approx 10^8$ CFU/ml, $P_0 \approx 2 \times 10^6$ to 8×10^6 PFU/ml). However, the fit between observed and predicted values decreased when the same parameter vector was used for predictions in cases with different initial densities (set 1 and set 4 of *L. mesenteroides* 1-A4). SSE(T) values were very high, indicative of an unsatisfactory fit between observed and predicted data, when the same parameter set was used to predict for all sets simultaneously, e.g., SSE(T) was equal to 515 for sets 1 to

TABLE 1. Results of parameter optimization for two or more data sets simultaneously for *L. mesenteroides* 1-A4 and phage 1-A4

Sets	α = γ (h^{-1})	*C* (CFU/ml)	*L* (h)	*B*	K_0 (ml/CFU/h)	K_1 (ml/CFU/h)	K_2 (ml/CFU/h)	K_3 (ml/CFU/h)	SSE(T)
1-2	0.35	9.89E + 08	0.30	25	2.07E-09	8.50E-10	4.38E-10	8.06E-11	4.60
1-3	0.36	8.76E + 08	0.36	19	3.33E-09	9.63E-10	5.05E-10	8.21E-11	17.35
1-4	0.74	8.89E + 08	0.36	22	5.12E-09	3.91E-09	2.22E-08	6.62E-10	515.00

TABLE 2. Coefficients of variation for parameters among different experimental conditions for *L. mesenteroides* 1-A4 and phage 1-A4

Set or parameter	$\alpha = \gamma$ (h^{-1})	C (CFU/ml)	L (h)	B	K_0 (ml/CFU/h)	K_1 (ml/CFU/h)	K_2 (ml/CFU/h)	K_3 (ml/CFU/h)
1	0.57	9.81E + 08	0.41	31	2.21E-09	1.07E-09	2.11E-10	1.00E-10
2	0.30	8.48E + 08	0.26	20	3.19E-09	9.36E-10	4.09E-10	7.86E-11
3	0.72	9.85E + 08	0.37	72	6.48E-08	5.15E-08	5.00E-08	1.55E-09
4	0.57	8.80E + 08	0.26	30	3.63E-09	8.82E-10	7.61E-10	3.10E-10
Mean value	0.54	9.23E + 08	0.33	38	1.84E-08	1.36E-08	1.28E-08	5.08E-10
SD	0.18	6.97E + 07	0.08	23	3.09E-08	2.53E-08	2.47E-08	6.99E-10
% CV	32	7.6	23	60	167	185	192	138

4 (Table 1). This suggested that some parameters may depend on the phage density and/or cell densities. The % CV was determined among four cases of phage-host system 1-A4 with different initial densities, and the results are shown in Table 2. In Table 2, parameter vectors containing average values of parameters after optimization for individual sets are given for phage-host system 1-A4. The overall mean and % CV are also shown in Table 2. The greatest coefficient of variation, greater than 100%, was found for the adsorption rate coefficient. The coefficient of variation for the burst size in the case of phage-host system 1-A4 was found to be 60%, which was relatively high compared to other parameters after the adsorption rate coefficient. This suggested that variation in phage-host kinetics for different initial conditions was largely due to changes in the adsorption rate coefficient. The adsorption rate coefficient values at different times (K_0, K_1, K_2, and K_3) for the *L. mesenteroides* 1-A4 data sets 1 to 4 were selected based on the data in Table 2. These data are shown in Fig. 2 to show the time dependence of the adsorption rate.

DISCUSSION

The results presented in Table 3 show that there were systematic differences between the parameters determined by model optimization and those determined from experiments. The growth rates calculated from parameter optimizations were higher than experimentally determined values for both *L. mesenteroides* 1-A4 and *L. pseudomesenteroides* 3-B11. This may be due to two factors. First, the observed values were calculated using optical density measurements, which may underestimate the growth rate. Secondly, the model may need further modifications. However, independent growth curves were obtained, and the growth rate was calculated using viable-colony counts analytically using the logistic function (data not shown), and it was found that these growth rates were higher than those measured from OD data and closer to predicted values. The growth rates of resistant bacteria were not significantly different from those of susceptible bacteria for both experimentally determined and numerically determined values of growth rates. This result was expected, as the two strains of bacteria are similar. The mean of experimentally determined values of burst size for phage-host system 1-A4 was found to be lower than the model-predicted value, but the large variation in both the observed and predicted burst sizes may explain this difference to some extent. Another possibility is that the delay differential equation presented in this paper assumes no variation in burst time or burst size. A more general model would include an integral term representing a distribution of latency periods and burst sizes.

Experimentally determined values of adsorption rate coefficients were similar to those that have been reported in the literature (9, 11, 15, 16, 17, 18, 19, 28). However, the values for the adsorption rate coefficient at time zero, obtained by parameter optimization, were found to vary, depending on the initial host cell density, with higher values of adsorption rates at lower initial cell densities for phage 1-A4. Large variation was observed in the numerically obtained adsorption rate coefficient at time zero compared to experimentally determined values. This may be attributed to the use of more or less similar initial conditions in the experimental determination of the adsorption rate coefficient.

It has been reported in the literature that the adsorption rate coefficient remains the same for various bacteria and phage concentrations (28). Adsorption rate coefficients have been calculated in the literature using high bacterial ($>10^6$ CFU/ml) and phage densities. The limitation in time for adsorption studies requires high bacterial concentrations ($>10^6$ CFU/ml) so that a decrease in free phage is measurable (9). However, there is no strong evidence that the adsorption rate coefficients

TABLE 3. Experimentally determined and predicted values of parameters and their statistics for phage-host systems 1-A4 and 3-B11[a]

Parameter	Value (mean ± SD)			
	Phage + host 1-A4		Phage + host 3-B11	
	From expt	Fitted to model	From expt	Fitted to model
Growth rate of susceptible cells (α) (h^{-1})	0.30 ± 0.006	0.54 ± 0.18	0.32 ± 0.01	0.40 ± 0.19
Growth rate of resistant cells (γ) (h^{-1})	0.30 ± 0.01	0.54 ± 0.18	0.27 ± 0.01	0.40 ± 0.19
Carrying capacity (C) (10^7 CFU/ml)	90.0 ± 13	92.3 ± 7.0	80 ± 8.7	100 ± 0.3
Latency (L) (h)	0.33 ± 0.07	0.33 ± 0.08	0.73 ± 0.10	0.60 ± 0.02
Burst size (B)	24 ± 13	38 ± 22	47 ± 13	41 ± 7.0
Adsorption rate coefficient (K_0) (10^{-9} ml/CFU/h)	55 ± 2	18.4 ± 30.9	50 ± 12	22.5 ± 12.6

[a] All of the bacterial parameters are consistent, as is the latency period, but different experimental conditions lead to variable burst size and adsorption rate.

are independent of the cell and phage concentrations. From the results of our validation kinetics studies performed with two *Leuconostoc* species and their specific phage, it has been found that the adsorption rate coefficient decreases with time and is dependent on the initial cell concentration. The results of parameter optimization studies strongly suggest that the adsorption rate coefficient may vary during phage-host interaction within wide limits. It is, of course, not a surprising observation, as the same kind of observation was made by Delbruck (9). The adsorption rate coefficient was found to vary 60-fold, depending on the physiological condition of the host (9). From the parameter optimization studies, there is a strong indication that the adsorption rate coefficient was higher when the initial cell concentration was lower, but surprisingly, it decreased during the course of the phage-host kinetics experiments, when the cell numbers were decreasing. This may be due to the production of metabolites by bacteria, leading to more successful infection due to resulting changes in the phage properties. Another possible explanation for this is that the adsorption rate constant may vary with the MOI; as phage-host kinetics proceeds, the MOI increases continuously. Variation in the adsorption rate constant with time and its dependence on the initial density of phage or host and/or MOI merit further investigation.

In the present study, only the adsorption rate was varied with time (using step functions); however, it is possible that other parameters may also change with time, depending on the physiological condition of the host. After adjusting for the adsorption rate constants based on the initial cell and phage densities, it was possible to achieve reasonably good predictions ($R^2 > 0.9$) for all the validation experiments, keeping other parameters specific to a particular phage-host system constant. Levin and Bull (17) also found that if they modified parameters associated with phage (i.e., adsorption and burst size) and allowed them to decline with time, their model better approximated the results.

Wang et al. (29) observed that the latent period varied, depending on the host density, and suggested that phage evolve a shorter latent period when the host density is high or the host quality is good. Longer latent periods are associated with larger burst sizes. The rate of phage adsorption decreases with the decrease in host quality. The latent period and the adsorption rate decrease with higher growth rates (1). All these studies suggest that kinetic parameters defining phage-host interaction also depend on the host cell density.

In the present study, the model was developed with several assumptions. It was assumed that kinetic parameters defining phage-host interactions were constant and independent of each other. In further modifications of the model, additional factors may be considered, such as the dependence of parameters on the growth rate of the cell. In parameter optimization, other parameters may be expressed as functions of the growth rate, and the results can be compared to the present results. The functional dependence of the latent period, burst size, and adsorption rate coefficient on the host growth rate is found in very few studies (25), and it may vary for different phage-host systems. The results of the model may be compared by varying the parameters, whose interdependence has to be determined, while holding other parameters constant. This approach may give an idea about the functional dependence of parameters on each other. In our study, the dependence of parameters on initial host and phage densities was tested by measuring the coefficient of variation between parameters among cases with different initial densities. Maximum variation was found in the adsorption rate, followed by the burst size. The adsorption rate coefficient can be described as a function of host density, and incorporating it in the model may make the model more robust. The model can then be used for a wider range of host concentrations using the same parameter set specific to a particular phage-host system. To understand the variation in the adsorption rate coefficient with time, adsorption experiments can be conducted at various initial cell and phage densities. The values of adsorption rate coefficients thus obtained can be correlated with cell density, phage density, and MOI to better understand the variation of the adsorption rate constant.

Preliminary data from experiments with starter cultures inoculated into commercial fermentations have shown that *L. mesenteroides* starter cultures inoculated at 10^6 CFU/g can reach 10^9 CFU/g (data not shown). Phage may be present in these commercial fermentation tanks, but it is likely that initial concentrations of phage would be at very low levels, on the order of 10^1 to 10^3 PFU/ml. In our laboratory experiments with phage, very low initial phage concentrations (10^2 to 10^3 PFU/ml), and 10^6-CFU/ml initial host cell concentrations, the phage killed the cells (Fig. 5d and 6b), although resistant cells remained. On the time scale of the commercial fermentations, the initial heterolactic fermentation phase with *L. mesenteroides* lasts about a week. During this time, the phage-resistant cells may dominate the *L. mesenteroides* population if a starter culture is used. In addition, the model was developed and validated using broth medium (MRS), which is more homogeneous than the commercial fermentation environment. The semisolid cabbage fermentation "medium" contains a heterogeneous packing density of the cabbage and salt. There could be many separate microenvironments, some of which may be free of phage. It is also possible that the parameters, such as the adsorption rate, differ from experimentally observed values in commercial sauerkraut fermentations. Further studies will include validation and possibly modifications of the model for use with commercial fermentations.

ACKNOWLEDGMENTS

We thank Roger McFeeters for helpful discussions and Dora Toler for secretarial assistance.

This investigation was supported in part by a research grant from Pickle Packers International, Inc. (Washington, D.C.).

Mention of a trademark or proprietary product does not constitute a guarantee or warranty of the product by the U.S. Department of Agriculture or North Carolina Agricultural Research Service, nor does it imply approval to the exclusion of other products that may be suitable.

REFERENCES

1. **Abedon, S. T., T. D. Herschler, and D. Stopar.** 2001. Bacteriophage latent period evolution as a response to resource availability. Appl. Environ. Microbiol. **67:**4233–4241.
2. **Adams, M. H.** 1959. Bacteriophages, p. 450–456. Interscience Publishers Inc., New York, N.Y.
3. **Beretta, E., and Y. Kuang.** 1998. Modeling and analysis of a marine bacteriophage infection. Math. Biosci. **149:**57–76.
4. **Breidt, F., K. A. Crowley, and H. P. Fleming.** 1995. Controlling cabbage fermentations with nisin and nisin-resistant *Leuconostoc mesenteroides*. Food Microbiol. **12:**109–116.
5. **Breidt, F., and H. P. Fleming.** 1998. Modeling of the competitive growth of

Listeria monocytogenes and *Lactococcus lactis* in vegetable broth. Appl. Environ. Microbiol. **64:**3159–3165.
6. **Breidt, F., T. L. Romick, and H. P. Fleming.** 1994. A rapid method for the determination of bacterial growth kinetics. J. Rapid Methods Autom. Microbiol. **3:**59–68.
7. **Buchanan, R. L.** 1991. Using spreadsheet software for predictive microbiology applications. J. Food Saf. **11:**123–134.
8. **Campbell, A.** 1961. Conditions for existence of bacteriophage. Evolution **15:**153–165.
9. **Delbruck, M.** 1940. Adsorption of bacteriophage under various physiological conditions of the host. J. Gen. Physiol. **23:**631–642.
10. **Delbruck, M.** 1940. The growth of bacteriophage and lysis of the host. J. Gen. Physiol. **23:**643–660.
11. **Ellis, E. L., and M. Delbruck.** 1939. The growth of bacteriophage. J. Gen. Physiol. **22:**365–384.
12. **Hadas, H., M. Einav, I. Fishov, and A. Zaritsky.** 1997. Bacteriophage T4 development depends on the physiology of its host *Escherichia coli*. Microbiology **143:**179–185.
13. **Harris, L. J., H. P. Fleming, and T. R. Klaenhammer.** 1992. Novel-paired starter culture system for sauerkraut, consisting of nisin-resistant *Leuconostoc mesenteroides* strain and a nisin-producing *Lactococcus lactis* strain. Appl. Environ. Microbiol. **58:**1484–1489.
14. **Kasman, M. L., A. Kasman, C. Westwater, J. Dolan, G. M. Schimidt, and J. S. Norris.** 2002. Overcoming the phage replication threshold: a mathematical model with implications for phage therapy. J. Virol. **76:**5557–5564.
15. **Kruegger, A. P.** 1931. Sorption of bacteriophage by living and dead susceptible bacteria. J. Gen. Physiol. **14:**493–516.
16. **Kruegger, A. P., and J. H. Northrop.** 1930. The kinetics of the bacterium bacteriophage reaction. J. Gen. Physiol. **14:**223–254.
17. **Levin, B. R., and J. J. Bull.** 1996. Phage therapy revisited: the population biology of a bacterial infection and its treatment with bacteriophage and antibiotics. Am. Nat. **147:**881–898.
18. **Levin, B. R., F. M. Stewart, and L. Chao.** 1977. Resource-limited growth, competition, and predation: a model and experimental studies with bacteria and bacteriophage. Am. Nat. **111:**3–24.
19. **Lu, Z., F. Breidt, H. P. Fleming, E. Altermann, and T. R. Klaenhammer.** 2003. Isolation and characterization of a *Lactobacillus plantarum* bacteriophage, ΦJL-1, from a cucumber fermentation. Int. J. Food Microbiol. **84:**225–235.
20. **Lu, Z., F. Breidt, V. Plengvidhya, and H. P. Fleming.** 2003. Bacteriophage ecology in commercial sauerkraut fermentations. Appl. Environ. Microbiol. **69:**3192–3202.
21. **Middleboe, M.** 2000. Bacterial growth and marine virus-host dynamics. Microb. Ecol. **40:**114–124.
22. **Mundt, J. O., W. F. Graham, and I. E. McCarty.** 1967. Spherical lactic acid-producing bacteria of southern-grown raw and processed vegetables. Appl. Microbiol. **15:**1303–1308.
23. **Payne, J. H., and A. A. Jansen.** 2000. Understanding bacteriophage therapy as a density dependent kinetic process. J. Theor. Biol. **208:**37–48.
24. **Pederson, C. S., and M. N. Albury.** 1969. The sauerkraut fermentation. New York State Agric. Exp. Sta. Tech. Bull. **824:**1–84.
25. **Rabinovitch, A., I. Fishov, H. Hadas, M. Einav, and A. Zaritsky.** 2002. Bacteriophage T4 development in *Escherichia coli* is growth rate dependent. J. Theor. Biol. **216:**1–4.
26. **Rabinovitch, A., H. Hadas, M. Einav, Z. Melamed, and A. Zaritsky.** 1998. Model for bacteriophage T4 development in *Escherichia coli*. J. Bacteriol. **181:**1677–1683.
27. **Rabinovitch, A., A. Zaritsky, I. Fishov, M. Einav, and H. Hadas.** 1999. Bacterial lysis by phage—a theoretical model. J. Theor. Biol. **201:**209–213.
28. **Schlesinger, M.** 1932. Adsorption of bacteriophage to homologous bacteria. Z. Hyg. Immunitatsforsch. **114:**149–160.
29. **Wang, I.-N., D. E. Dykhuizen, and L. B. Slobodkin.** 1996. The evolution of phage lysis timing. Evol. Ecol. **10:**545–558.
30. **Yoon, S.-S., R. Barrangou-Poueys, F. Breidt, Jr., T. R. Klaenhammer, and H. P. Fleming.** 2002. Isolation and characterization of bacteriophages from fermenting sauerkraut. Appl. Environ. Microbiol. **68:**973–976.